Polymer Vol. 39 No. 24 pp. 6067–6072, 1998
0032-3861/98/$ – see front matter

PII: S0032-3861(98)00104-9

A new binary system exhibiting simultaneous crystallization and spinodal decomposition: poly(ethylene-2,6-naphthalenedicarboxylate)/poly(ether imide) blend

Hsin-Lung Chen[a,*], Jenn Chiu Hwang[b] and Rong-Chung Wang[b]
[a]*Department of Chemical Engineering, National Tsing Hua University, Hsin-Chu, Taiwan 30034, ROC*
[b]*Department of Chemical Engineering, Yuan Ze University, Nei-Li, Taoyuan, Taiwan, ROC*
(Received 29 October 1997; revised 16 January 1998; accepted 26 January 1998)

The phase behaviour and crystallization of poly(ethylene-2,6-naphthalenedicarboxylate) (PEN)/poly(ether imide) (PEI) blends were investigated. PEN and PEI were miscible in the melt over the entire composition range. A PEI-rich phase containing *ca*. 80 wt.% of PEI was identified after the crystallization of PEN below 240°C. This observed composition deviated from the composition calculated by assuming a simple liquid–solid phase separation. Morphological observation by optical microscopy revealed simultaneous occurrence of spinodal decomposition and crystallization, where modulated structure was locked in by the crystallization of PEN. A UCST phase diagram with the binodal line located below the equilibrium melting point was identified. Investigation on the multiple melting behaviour showed that recrystallization of PEN following the initial melting was hindered due to the remixing between PEN and PEI. Despite the occurrence of spinodal decomposition, the crystallization rate of PEN still dropped with increasing initial PEI composition.

(Keywords: PEN; poly(ether imide); blend)

INTRODUCTION

Liquid–liquid phase separation and crystallization in polymer blends are of great interests because they may create a wide variety of morphology and properties. Most studies concerning phase separation and crystallization have dealt with either one of the processes, while little attention has been directed to the pattern formation where both may take place simultaneously[1–11]. As these two processes occur at the same time, liquid–liquid phase separation can compete with crystallization in producing its own morphology and the final blend morphology is dependent on the outcome of such a competition. The morphology thus created may be unique in that it is not attainable by either process alone.

There are two possibilities for a blend to exhibit competitive liquid–liquid phase separation and crystallization. (1) The blend is immiscible above and below the melting point (M.P.). An unstable morphology with interconnected domains or small domain droplets may be formed initially by mechanical mixing or solution blending. As the blend is immediately brought to a crystallization temperature (T_c), the rearrangement of initially formed domains to reach the stable phase-separated morphology will proceed simultaneously with crystallization. Hashimoto and co-workers have studied the competition between spinodal decomposition and crystallization in isotactic polypropylene (i-PP)/ethylene-propylene copolymer (EPR) blends[2,4]. This binary pair was immiscible and interconnected domains were formed after solvent cast. The interconnected domains gradually coarsened in the melt but they can be locked in by allowing i-PP to crystallize at temperatures below M.P. (2) The blend is miscible above M.P., but displays a miscibility gap below M.P. This happens when the M.P. depression curve intersects a UCST phase diagram or when the UCST phase diagram is located below the M.P. depression curve. The blend is homogeneous above the critical point and M.P. Below M.P., liquid–liquid phase separation proceeds simultaneously with crystallization. Liquid–liquid phase separation has no equilibrium significance below M.P., since crystallization is the thermodynamically favourable process. But due to the nucleation barrier associated with polymer crystallization, liquid–liquid phase separation via the mechanism of spinodal decomposition could precede the crystallization[6]. The UCST phase diagram of poly(ϵ-caprolactone) (PCL)/polystyrene (PS) oligomer blends has been found to intersect the M.P. depression curve such that competitive liquid–liquid phase separation and crystallization was observed below M.P.[1,5,7]. Poly(vinylidene fluoride) (PVF_2)/poly(methyl methacrylate) (PMMA) blends have also been reported to display a UCST phase diagram below M.P.[3,8]. In the previous studies, we have explored two systems, poly(ethylene terephthalate) (PET)/PEI and poly(butylene terephthalate) (PBT)/PEI, which exhibited simultaneous phase separation and crystallization below M.P.[10,11].

Another system of interest is the blend of PEI with

* To whom correspondence should be addressed

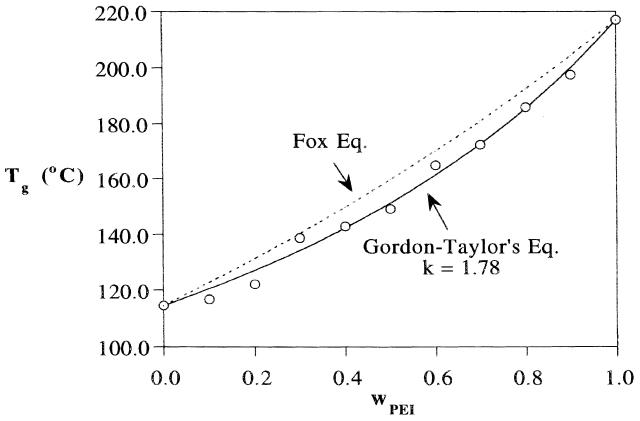

Figure 1 Composition dependence of T_g of amorphous PEN/PEI blends. The dashed line is the prediction by Fox equation and the solid line is the fit by Gordon–Taylor's equation

another aromatic polyester, poly(ethylene-2,6-naphthalene-dicarboxylate) (PEN). PEN is a semicrystalline polymer with the glass transition temperature (T_g) and M.P. around 115 and 280°C, respectively. Both T_g and M.P. of PEN are higher than those of PET since the phenylene moiety in PET was replaced by the naphthalene group in PEN. Because of similarity between the chemical structures of PEN and PET, it is of interest to blend PEN with PEI and see if this binary pair can offer a new system displaying competitive phase separation and crystallization. In this study, the phase behaviour of PEN/PEI blends in both the melt and the semicrystalline state are reported. The effect of blending with PEI on the crystallizability, melting behaviour, and crystallization kinetics of PEN will also be described.

EXPERIMENTAL

PEN used in this study was supplied by the Far Eastern Textiles Co. Ltd., Taiwan. PEI was obtained from General Electric (GE, Ultem 1000), and its molecular weights were $M_n = 12\,000$ and $M_w = 30\,000$.

Blending of PEN and PEI was carried out by solution precipitation. PEN and PEI were dissolved in dichloroacetic acid at room temperature, yielding a 4 wt.% solution. The blends were subsequently recovered by precipitating them in 20-fold excess volume of water. The blends were washed with a large amount of water and then dried in vacuo at 100°C for 5 days.

Thermal transitions of the blends were measured with a Perkin-Elmer DSC-7 differential scanning calorimeter. For the T_g measurement, the sample was heated to 300°C and annealed for 15 min to erase previous thermal history. The sample was then quickly quenched into liquid nitrogen and d.s.c. scan was conducted at 20°C/min to record the glass transition region. As to the melting behaviour study, the sample was annealed at 300°C followed by cooling at *ca*. 160°C/min to the desired crystallization temperatures. The d.s.c. scan was conducted at 20°C/min after 11 h of crystallization. For the study of isothermal crystallization kinetics, the sample was annealed at 300°C for 3 min followed by cooling at *ca*. 160°C/min to the crystallization temperature, and the isothermal crystallization exotherm was recorded.

The morphologies of PEN/PEI blends were observed by a Nikon FX-A cross-polarized optical microscope. The sample was first melted on a Linkam HFS91 hot stage at 300°C for 3 min. The sample was then quickly transferred to another hot stage equilibrated at the desired crystallization temperature, where the resultant morphology was observed.

RESULTS AND DISCUSSION

Phase behaviour

Miscibility of polymer blends is typically judged through the observation of glass transition temperature. *Figure 1* plots the T_g against composition for PEN/PEI blends quenched from melt. A single T_g is identified over the entire composition and T_g increases monotonically with increasing PEI composition. This indicates the miscibility between PEN and PEI in the melt. The T_g–composition relationship deviates from the conventional Fox equation[12]:

$$\frac{1}{T_g} = \frac{w_1}{T_{g1}} + \frac{w_2}{T_{g2}} \tag{1}$$

But the Gordon–Taylor's equation provides a satisfactory description for the composition variation of T_g[13]:

$$T_g = \frac{w_1 T_{g1} + k w T_{g2}}{w_1 + k w_2} \tag{2}$$

with the adjustable parameter $k = 1.78$. The fit of Gordon–Taylor's equation to the experimental T_g indicates a fairly weak interaction between PEN and PEI[14].

Since the combinatorial entropy of mixing is negligible, the presence of favourable interaction is inevitable for miscibility in polymer blends. The favourable interaction between PEN and PEI may be too weak to be resolvable by the composition dependence of T_g. The aromatic moieties in PEN, PET, and PBT are most likely to contribute to the favourable (but not strong) interactions with PEI, because immiscibility was found for the blends of PEI with poly(ethylene succinate), a polyester with the chemical structure of replacing the naphthalene moiety in PEN by ethylene (CH_2CH_2) group.

One objective of this study is to reveal whether PEN/PEI blends also display simultaneous liquid–liquid phase separation and crystallization. Some critical information on the composition distribution may be revealed by observing the T_g of the blends after crystallization. *Figures 2 and 3* show the glass transition regions of PEN/PEI blends after crystallizing at 245 and 230°C for 11 h, respectively. The T_g still displays a monotonic increase with PEI composition after crystallization at 245°C. The situation becomes different for $T_c = 230$°C, where a T_g located at *ca*. 185°C is identified and this T_g is relatively independent of initial blend composition. According to the T_g–composition curve in *Figure 1*, a T_g of 185°C corresponds to the glass transition of the amorphous region containing *ca*. 80 wt.% PEI. This means a strong segregation of PEI had occurred after the crystallization of PEN. Although crystallization of PEN must be accompanied with the segregation of PEI, it seems quite unlikely that the observed segregation was induced solely by such a liquid–solid phase separation considering the very high observed PEI concentration. Suppose the segregation of PEI was induced by crystallization such that PEI was continuously expelled to the remaining miscible melt during crystallization, the composition of the miscible amorphous phase may then be estimated from the simple mass balance relationship:

$$w_{PEI} = \frac{w^0_{PEI}}{w^0_{PEI} + (w^0_{PEN} - w_c)} = \frac{w^0_{PEI}}{1 - \Delta h_f / \Delta h^0_f} \tag{3}$$

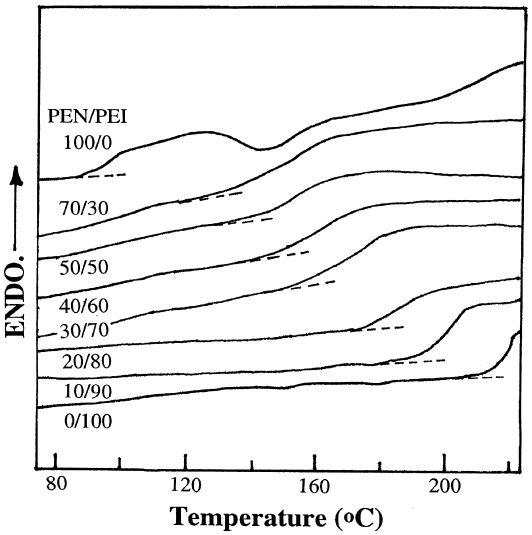

Figure 2 Glass transition regions of PEN/PEI blends subjected to crystallization at 245°C for 11 h

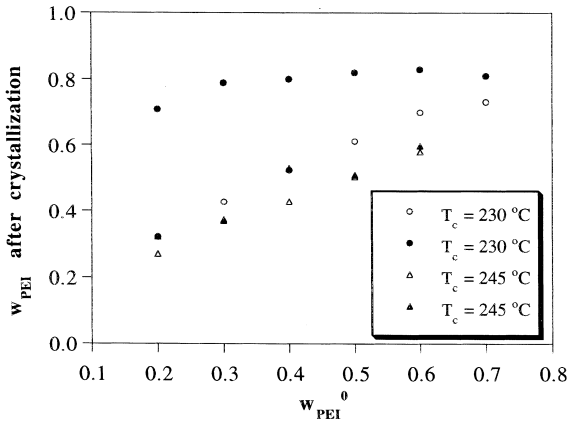

Figure 4 Comparisons between the PEI compositions calculated by equation (3) and that determined from the observed T_g for $T_c = 230$ and 245°C. The open symbols are the calculated values and the filled symbols are the observed values. Good agreement is found for $T_c = 245$°C, but the observed compositions are significantly higher than the calculated values for $T_c = 230$°C

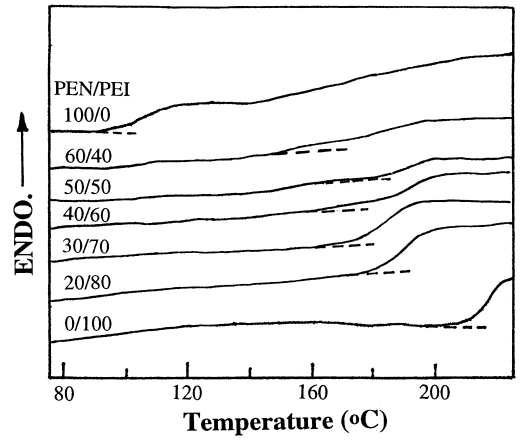

Figure 3 Glass transition regions of PEN/PEI blends subjected to crystallization at 230°C for 11 h

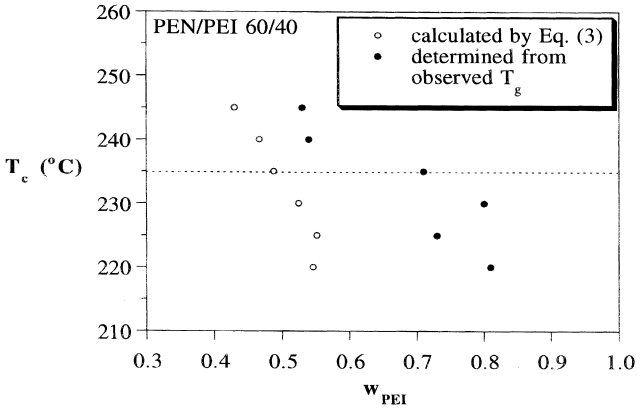

Figure 5 Comparisons between the PEI compositions calculated by equation (3) and that determined from the observed T_g for PEN/PEI 60/40 blend crystallized at various temperatures. Good agreement is found for $T_c \geq 240$°C, while the observed compositions are about 20% higher than the calculated values for $T_c \leq 235$°C

where w^0_{PEI} and w^0_{PEN} are the initial weight fractions of PEI and PEN, respectively, w_c is the degree of crystallinity of PEN, Δh_f is the measured enthalpy of melting, and $\Delta h^0_f = 103.7$ J/g[15], the bulk enthalpy of melting. In *Figure 4*, the amorphous composition computed from equation (3) is compared with that evaluated from the observed T_g for PEN/PEI crystallized at 230 and 245°C. The calculated compositions agree quite well with the observed compositions for $T_c = 245$°C, while the observed compositions are significantly higher than the calculated values for $T_c = 230$°C. *Figure 5* plots the observed and calculated compositions for 60/40 blend crystallized at various temperatures for 11 h. For T_c higher than 235°C, the calculated compositions show better agreement with the observed values, but the observed PEI composition is always about 20% higher than the calculated value for $T_c \leq 235$°C. The observations in *Figures 4 and 5* suggest that, above certain temperatures, the segregation of PEI was induced by the process of liquid–solid phase separation. But the observed strong PEI segregation may not be predicted by such a phase separation below certain temperatures.

In order to gain further details on the nature of the PEI segregation, the morphology of PEN/PEI blends after crystallization was observed by optical microscopy. *Figure 6* displays the morphological development of PEN/PEI 60/40 blend crystallized at 230°C. The blend shows a state homogeneous melt without any morphological texture when just cooled to 230°C. A coarsening texture formed as the crystallization proceeded. Unlike the typical spherulitic structure, the morphology is characterized by the interconnected domains which appear like the modulated structure developed in spinodal decomposition. *Figure 7* compares the morphology of pure PEN with that of the blends crystallized at 220°C. Pure PEN displays the conventional spherulitic texture, while modulated morphology was clearly identified for the blends. In conjunction with the observed strong segregation of PEI, it is concluded that crystallization of PEN was coupled with a liquid–liquid phase separation proceeding via spinodal decomposition. During the crystallization of PEN, spinodal decomposition and crystallization were competing in creating its own morphology. Hashimoto and co-workers have found that if the crystallization was sufficiently rapid, the modulated morphology may be locked in by crystallization[2,4]. The morphological development of PEN/PEI blends appears to

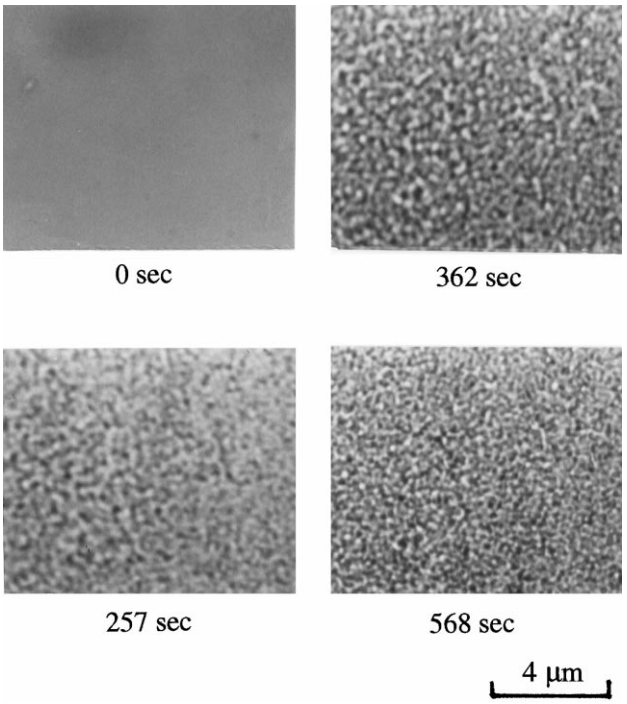

Figure 6 Morphological development viewed under optical microscopy for PEN/PEI 60/40 blend at 230°C. The time of crystallization is indicated in the figure. A modulated morphology created by spinodal decomposition is observed

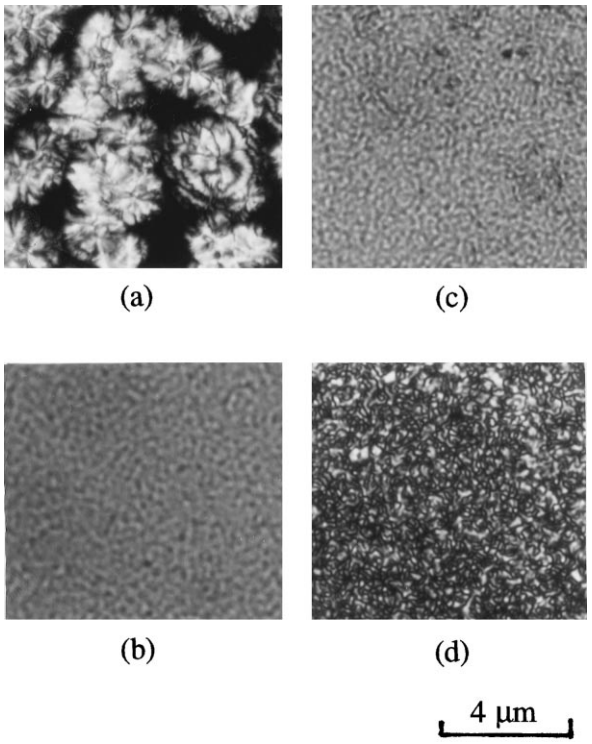

Figure 7 Optical micrographs showing the morphologies of (a) pure PEN (b) PEN/PEI 80/20, (c) 60/40, and (d) 60/40 blends at 230°C. Micrographs (a) and (d) were viewed under cross polarization

be such a case where the crystallization of PEN was fast enough to preserve the modulated morphology induced by spinodal decomposition.

As has been indicated, coupling between crystallization and liquid–liquid phase separation occurs when the binodal

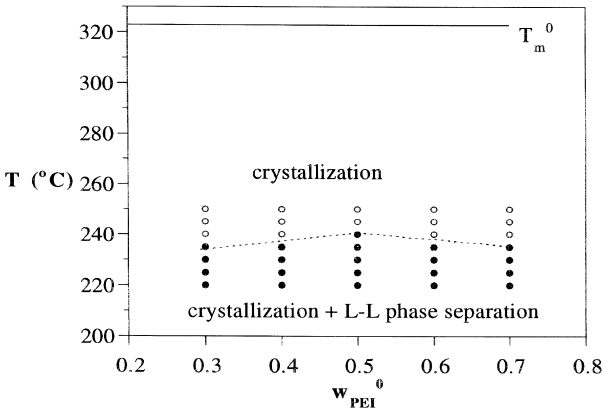

Figure 8 Phase diagram of PEN/PEI blend. The filled symbol stands for the observation of simultaneous liquid–liquid phase separation and crystallization, while the open symbol denotes the observation of crystallization only

curves intersect the M.P. depression curve, or when the miscibility gap locates below the M.P. depression curve. The phase diagram of PEN/PEI blends was evaluated by observing the resultant morphology for various blend compositions at different temperatures. The result is shown in *Figure 8*. A UCST phase diagram with the binodal curve located blow the equilibrium M.P. is identified. All PEN/PEI blends were in the form of miscible melt above M.P.; within the temperature and composition range bounded by the dashed line, crystallization was found to proceed simultaneously with liquid–liquid phase separation. Since the composition of the PEI-rich phase evaluated from the observed T_g is around 0.8, irrespective of the initial composition, this composition may correspond to the binodal composition of the PEI-rich phase. As to the binodal composition of PEN-rich phase, the T_g of this phase could not be identified because crystallization should have taken place within this phase due to high PEN concentration. The occurrence of crystallization could further shift the composition into the unstable region and spinodal decomposition was induced again; eventually only the T_g corresponding to PEI-rich phase was identified. It is noted that the miscibility gap determined by the present methods (namely, optical microscopy and thermal analysis) may locate slightly lower than that measured by light scattering, since light scattering can detect composition fluctuation arising from liquid–liquid phase separation more sensitively than the methods used here[8].

Crystallization behaviour

The effects of blending with PEI on the crystallizability, melting behaviour, and crystallization kinetics of PEN were also evaluated. *Figure 9* plots the degree of crystallinity against the blend composition. The crystallinities shown in *Figure 9* have been normalized by the weight fraction of PEN to stand for the amount of crystals formed per unit weight of PEN. The normalized crystallinity is seen to decrease with increasing PEI composition, which means that the crystallizability of PEN was retarded upon blending with PEI. The decrease in PEN molecular mobility upon blending is likely to contribute to the crystallinity reduction.

PEN may exhibit multiple melting endotherms after isothermal crystallization. Similar to PET and PBT, such a multiple melting behaviour may be associated with the occurrence of melting, recrystallization, and remelting in the melting region[16,17]. *Figure 10* displays the melting

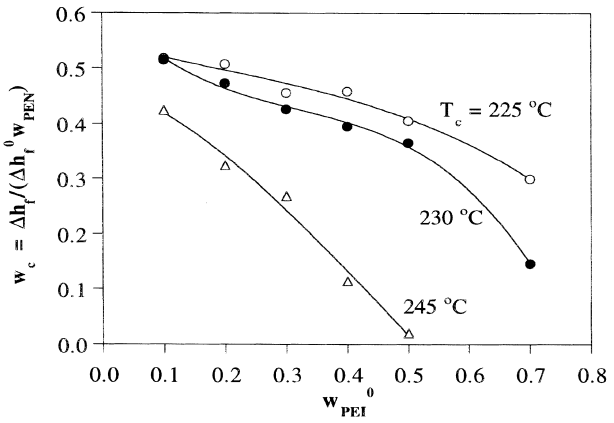

Figure 9 Variation of the normalized crystallinity with composition of PEN/PEI blends

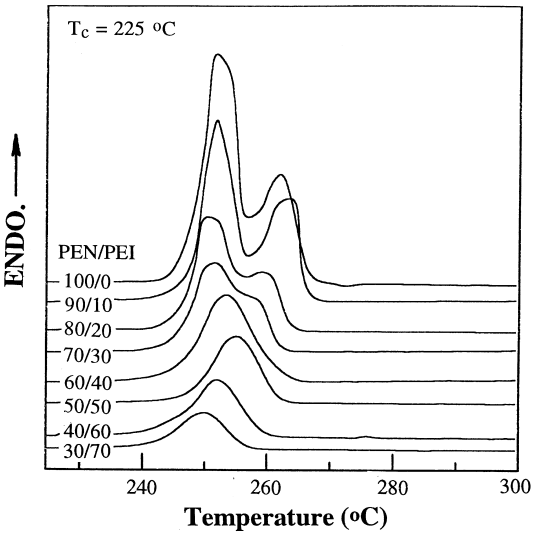

Figure 12 Melting endotherms of PEN/PEI blends subjected to crystallization at 225°C for 11 h

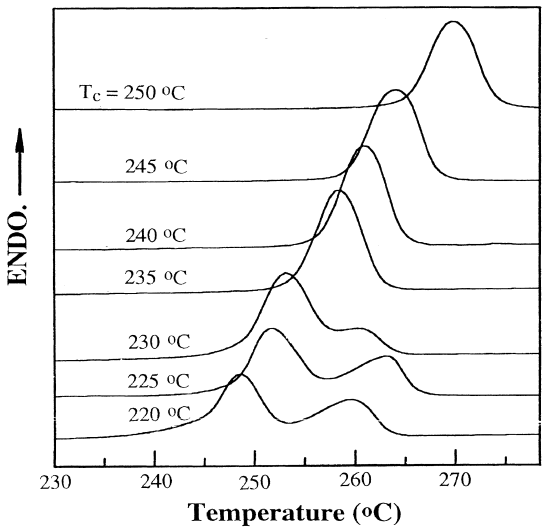

Figure 10 Melting endotherms of PEN/PEI 90/10 blend subjected to crystallization at various temperatures for 11 h. The crystallization temperatures are indicated in the figure

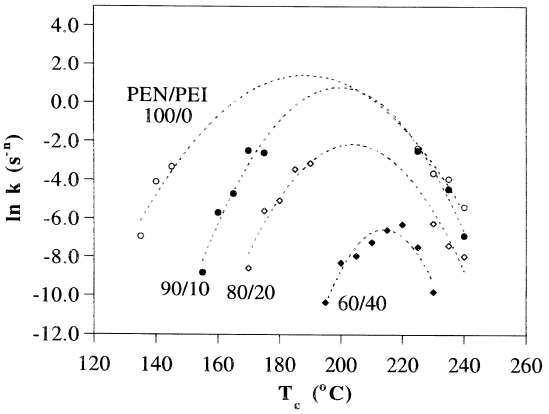

Figure 13 Logarithmic crystallization rate constants at different crystallization temperatures. The crystallization rate decreases with increasing PEI composition at a given T_c

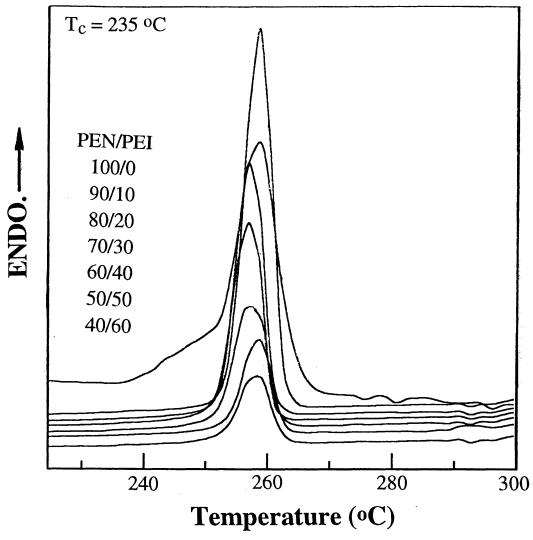

Figure 11 Melting endotherms of PEN/PEI blends subjected to crystallization at 235°C for 11 h

endotherms of PEN/PEI 90/10 blend subjected to crystallization at various T_c values for 11 h. Only one endotherm is observed for $T_c \geq 235$°C, whereas two melting peaks are identified with a smaller endotherm developed at *ca*. 260°C for $T_c \leq 230$°C. The magnitude of the second endotherm relative to that of the first endotherm becomes larger for lower T_c. The ability for a polymer to undergo recrystallization after initial melting is related to the degree of undercooling given by $(T_m^0 - T_m)$ with T_m^0 being the equilibrium M.P. and T_m the observed M.P.[17]. The larger the degree of undercooling, the greater the tendency towards recrystallization. The crystals formed at a higher T_c have a higher T_m and hence a lower driving force towards recrystallization. Consequently, recrystallization is negligible for $T_c \geq 235$°C. On the other hand, the crystals formed at $T_c \leq 230$°C had a lower T_m and thus a stronger tendency towards recrystallization. Two melting endotherms were then observed and the magnitude of the second endotherm became larger for lower T_c.

The melting behaviour of PEN was found to be influenced by blending with PEI. *Figures 11 and 12* show the melting endotherms of PEN/PEI blends subjected to prior crystallizations at 235 and 225°C for 11 h, respectively.

For $T_c = 235$°C for which PEN did not exhibit significant recrystallization in the melting region, blending does not exert any strong perturbation on the shape of melting endotherms. On the other hand, differences in the shapes of melting endotherms are observed for $T_c = 225$°C. Two melting endotherms are observed for pure PEN. With increasing PEI composition, the second endotherm located at *ca*. 265°C gradually diminishes and only one endotherm is observed when the PEI composition exceeds 30 wt.%. This phenomenon clearly indicates that the recrystallization of PEN was hindered upon blending with PEI. The hindrance was stronger in blends with higher PEI composition. The hindrance of recrystallization may be ascribed to the remixing between PEN and PEI after initial melting. Since the majority of the melting range is located in the one-phase region in the phase diagram of *Figure 8*, when PEN crystals melted, the melted PEN would remix with the remaining miscible melt. The subsequent recrystallization required the diffusion of PEN segments out of the melt; such a diffusion was impeded by PEI and recrystallization was hindered.

As spinodal decomposition preceded the crystallization, the kinetics of crystallization over the spinodal domains may be different from the case where no such a coupling existed. For example, crystallization rate may be promoted if nucleation can occur preferentially on the domain interface[18]. The effect of blending on the bulk crystallization kinetics of pen was investigated by avrami analysis:

$$\ln\{-\ln[1-x_c(t)]\} = \ln k + n \ln t \qquad (4)$$

where $x_c(t)$ is the relative crystallinity accumulated as of time t, k is the crystallization rate constant, and n is the Avrami exponent. *Figure 13* plots the logarithmic rate constants against T_c for various PEN/PEI blend compositions. The crystallization rate decreases with increasing PEI composition at a given T_c, so promotion in crystallization rate is not observed. This means that the nucleation at the domain interface, if it took place, did not play a major role in controlling the crystallization rate of PEN.

During spinodal decomposition, change of compositions took place continuously with one phase continuing to enrich PEN content and the other to enrich PEI content. Crystallization should proceed preferentially within PEN-enriched phase. For one extreme case where crystallization completes before the occurrence of spinodal decomposition, the crystallization kinetics is determined by the initial blend composition and increasing PEI composition will result in decreasing crystallization rate. This situation is unlikely because crystallization needs to overcome a nucleation barrier, whereas spinodal decomposition can be induced with infinitesimal fluctuations such that it should precede crystallization[6]. For the other extreme, where crystallization starts to take place after the binodal compositions have been reached, then crystallization should proceed at the same rate irrespective of the initial composition. The decrease of crystallization rate with increasing initial PEI composition in *Figure 13* suggests that the crystallization of PEN should belong to the intermediate case where it did not lag behind the composition shift arising from spinodal decomposition considerably. The PEI composition within the PEN-enriched phase was still higher in the blend with higher initial PEI composition, such that the crystallization rate is slower.

CONCLUSIONS

A new binary system, PEN/PEI, exhibiting simultaneous liquid–liquid phase separation and crystallization has been discovered in this study. PEN and PEI were miscible in the melt but a UCST phase diagram was located below M.P. Crystallization of PEN was coupled with spinodal decomposition, where modulated spinodal morphology was locked in by the crystallization of PEN. Blending with PEI depressed the crystallizability of PEN. The melting behaviour of PEN was also affected by blending. The recrystallization following the initial melting was impeded due to remixing. Although composition shift arising from spinodal decomposition was taking place simultaneously with crystallization, the crystallization rate of PEN still decreased with increasing PEI composition.

ACKNOWLEDGEMENTS

The support of this work by the National Science Council of the Republic of China under grant NSC 87-2216-E-007-046 is gratefully acknowledged.

REFERENCES

1. Tanaka, H. and Nishi, T., *Phys. Rev. Lett.*, 1985, **55**, 1102.
2. Inaba, N., Sato, K., Suzuki, S. and Hashimoto, T., *Macromolecules*, 1986, **19**, 1690.
3. Saito, H., Fujita, Y. and Inoue, T., *Polymer J.*, 1987, **19**, 405.
4. Inaba, N., Yamada, T., Suzuki, S. and Hashimoto, T., *Macromolecules*, 1988, **21**, 407.
5. Tanaka, H. and Nishi, T., *Phys. Rev. A*, 1989, **39**, 783.
6. Burghardt, W. R., *Macromolecules*, 1989, **22**, 2482.
7. Li, Y. and Jungnickel, B.-J., *Polymer*, 1993, **34**, 9.
8. Tomura, H., Saito, H. and Inoue, T., *Macromolecules*, 1992, **25**, 1611.
9. Cham, P. M., Lee, T. H. and Marand, H., *Macromolecules*, 1994, **27**, 4263.
10. Chen, H.-L., *Macromolecules*, 1995, **28**, 2845.
11. Chen, H.-L., Hwang, J. C., Chen, C.-C., Wang, R.-C., Fang, D.-M. and Tsai, M.-J., *Polymer*, 1997, **38**, 2742.
12. Fox, T. G., *Bull. Am. Phys. Soc.*, 1956, **1**, 123.
13. Gordon, M. and Taylor, J. S., *J. Appl. Chem.*, 1952, **2**, 495.
14. Lin, A. A., Kwei, T. K. and Reisen, A., *Macromolecules*, 1989, **22**, 4112.
15. Cheng, S. Z. D. and Wunderlich, B., *Macromolecules*, 1988, **21**, 789.
16. Nichols, M. E. and Robertson, R. E., *J. Polym. Sci. Polym. Phys. Ed.*, 1992, **30**, 755.
17. Chen, H.-L., Hwang, J. C. and Chen, C.-C., *Polymer*, 1996, **37**, 5461.
18. Stein, R. S., *Mat. Res. Soc. Symp. Proc.*, 1994, **321**, 531.